

Small Signal Stability Analysis of the Wind Farm Integrated Power System in Penghu Island

Shao-Hong Tsai*, Chung-Huo Lin, Yi-Hsiang Tseng

Department of Electrical Engineering, Hwa-Hsia University of Technology, Taiwan, R.O.C.

*Corresponding Email: shtsai@cc.hwh.edu.tw

Abstract :Modern wind turbine technology has been a great improvement over the past few decades, leading to large scale wind power penetration. The increasing penetration of wind power resulted in emphasizing the importance of reliable and stable operation of power systems, especially in an isolated small-scale power system. This paper describes the impact of full-load converter interfaced wind generators on power system oscillations. Eigenvalue analysis and participation factors are carried out under variant wind power penetration levels to investigate the small signal stability of the isolated small-scale power system in Penghu Island.

Keywords: Small Signal Stability, Wind Farm, Eigenvalues, Participation Factors

I. Introduction

Renewable generation resources have become an increasingly popular alternative to conventional fossil fuel based generation over the past few decades. Among them wind power is the most rapidly developing electricity generation source, and the installed wind power capacity has been reached around 396 GW worldwide by the end of 2015 [1]. As wind energy is increasingly integrated into power systems, the reliability and stability of wind power generation system has been getting more attention from researchers owing to the fact that the operational conditions and characteristics of wind generators are very different from those of traditional synchronous generators [2].

Many special intensive researches for the small signal stability of wind farms connected to power systems have been proposed in the last decade, which devoted to modelling and analysis of wind turbines with variant types of generators. In [3], models of the three most important actual wind turbine concepts: a constant speed wind turbine with squirrel cage induction generator (SCIG), a variable speed wind turbine with doubly fed induction generator (DFIG), and a variable speed wind turbine with a direct drive synchronous generator (DDSG), were described and a method was presented to calculate the initial conditions of dynamic models of the three concepts. The modelling and small signal analysis of a grid connected DFIG was presented in [4], and eigenvalue and participation factors analysis of the linearized models were carried out. Results show that the stator current, turbine speed, twist angle, generator speed and rotor flux q-component are the main responsible for oscillating modes. In [5], a damping controller on the different modes of operation for the DFIG

based wind generation system was implemented, and an optimal algorithm for coordinated tuning of the damping controller to enhance the damping of the oscillatory modes was presented. The results show that the damping controller gives effective damping out the low-frequency oscillations. In [6, 7], the small signal analysis considering converter and pitch controllers was studied, and a model simplification of the DFIG wind turbine was presented to promote dynamic performance. An optimal controller design using multi-objective differential evolution (DE) was presented in [8]. Results show that using the coordinated tuning of the controllers' parameters of the rotor and grid side converters can effectively improve the damping performance and the stability margin of the DFIG wind turbine. In [9, 10], the impact of full-load converter interfaced wind turbines on power system small signal stability was studied. The results have shown that there is a general decoupling between the grid dynamics and the wind turbine mechanical system by the full-load converter, that is, it implies that the system oscillatory modes of the wind turbine mechanical system have less effective than those of the synchronous generators' mechanical system. The eigenvalue analysis based on models considering the controllers' parameters of a wind turbine with direct drive PMSG was evaluated in [11, 12]. Mode shape and participation factors analysis reveals the origin of different modes and controller's parameters can be chosen properly. In this paper, the small signal stability analysis of an isolated small-scale power system with full-load converter interfaced wind turbines is presented to investigate the impact of different wind turbine penetration on power system behavior.

II. Small Signal Stability

Power system dynamics can be described by a set of nonlinear differential equations together with a set of algebraic equations (DAE) of the following form [13]:

$$\begin{cases} \dot{x} = f(x, y, u) \\ 0 = g(x, y, u) \end{cases} \quad (1)$$

where x is the vector of the state variables, y is the vector of the algebraic variables, and u is the vector of system parameters, e.g., the load level of the whole system. In the case of small signal stability analysis, (1) is linearized around an equilibrium point to yield the linearized DAE model as:

$$\begin{bmatrix} \Delta\dot{x} \\ 0 \end{bmatrix} = \begin{bmatrix} f_x(u) & f_y(u) \\ g_x(u) & g_y(u) \end{bmatrix} \begin{bmatrix} \Delta x \\ \Delta y \end{bmatrix} \equiv A_{total} \begin{bmatrix} \Delta x \\ \Delta y \end{bmatrix} \quad (2)$$

where A_{total} is the total system Jacobian matrix, Δ denotes an incremental change in steady state value. By eliminating the

algebraic variables y in (2), the equivalent system state matrix can be formulated as $A = f_x(u) - f_y(u) g_y^{-1}(u) g_x(u)$. The small signal stability of the nonlinear system (1) in the neighborhood of the equilibrium point can be analyzed by inspecting the eigenvalues of the linearized system (2); e.g., all of the eigenvalues of the system state matrix A should have negative real parts to maintain the stability. Accordingly, eigenvalues close to the imaginary axis of the complex plane are the critical eigenvalues of interest to analyze the stability of power system oscillations.

Equation (3) describes that the critical eigenvalues and corresponding eigenvectors construct a dominant invariant subspace with respect to the entire eigenspace of system state matrix.

$$\begin{aligned} A(u)V(u) &= V(u)\Lambda(u) \\ U(u)A(u) &= \Lambda(u)U(u) \end{aligned} \quad (3)$$

where the column vectors, known as right eigenvectors, in $V(u)$ and the column vectors, known as left eigenvectors, in $U(u)$ are the basis in the invariant subspace, and the eigenvalues of $\Lambda(u)$ are a fraction of the corresponding eigenvalues in the full matrix $A(u)$.

The participation matrix P combines the right and left eigenvectors as a measure of the relation between the states and the modes [13].

$$P = [p_1 \ p_2 \ \cdots \ p_n] \quad (4)$$

with

$$p_i = \begin{bmatrix} p_{1i} \\ p_{2i} \\ \vdots \\ p_{ni} \end{bmatrix} = \begin{bmatrix} v_{1i}u_{i1} \\ v_{2i}u_{i2} \\ \vdots \\ v_{ni}u_{in} \end{bmatrix}$$

where p_i is the participation factor of mode i . For the i^{th} eigenvalue ($\lambda_i = \alpha_i \pm \beta_i$), the frequency of oscillation in Hz is given by (5), and the damping ratio is given by (6), which determines the rate of decay of the amplitude of the oscillation.

$$\zeta_i = \frac{-\alpha_i}{\sqrt{\alpha_i^2 + \beta_i^2}} \quad (5)$$

$$f_i = \frac{\beta_i}{2\pi} \quad (6)$$

III. Description of the Penghu Power System

Penghu archipelago, covering an area of 127 square kilometers, is located in the Taiwan Strait between mainland China and Taiwan Island. The Penghu system shown in Fig. 1 is a typical weak and isolated power system in which the main power generation located at Chien-shan power plant consists of 12 diesel generators, bring total installed capacity up to 129.77 MW. Three wind farms, namely Chung-tun WF no.1, Chung-tun WF no.2 and Husi WF, are integrated into the Husi substation and have total installed capacity of 10.2 MW. The above mentioned power generation provides electricity consumption by feeders connected to Magong and Husi

substations. The demand loads in Penghu system vary depending on weather conditions and in general can be formulated as four operating scenarios, i.e., summer peak load (SP), summer light load (SL), winter peak load (WP) and winter light load (WL) for research purpose. For small signal analysis, Table 1 shows the models of the diesel generators, excitors and speed governors, and the controllers used in the three wind farms. Table 2 shows the total state variables and demand loads of the four operating scenarios, and corresponding wind power generation for the simulation conditions of this study. Comparing to the diesel generators, the wind generators are expected to have as much generation as possible owing to their lower generation costs. Therefore, all wind generators operate under the assumed rated power output so as to have a high penetration of wind power in Penghu power system, especially at light load conditions.

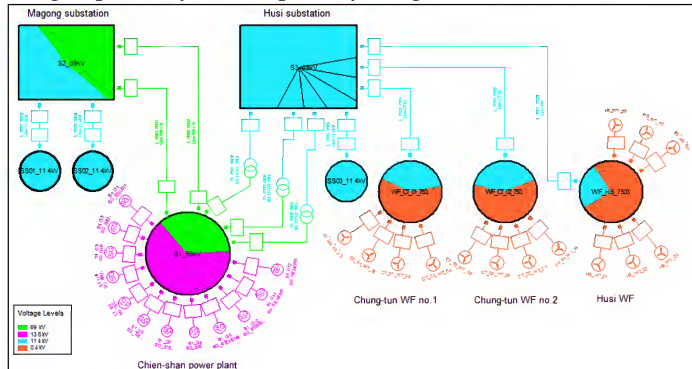


Fig. 1: Single-line diagram of the Penghu power system

Models	Generator	Exciter	Speed governor
generators #1 -#4	GENSAL	IEEEX2	DEGOV1
generators #5 -#12	GENSAL	ESAC8B	DEGOV1
wind farms	full-load converter interfaced wind turbine		
WF controllers	PQ, current and over frequency power reduction controllers		

Table 1: Models of diesel generators and controllers of wind farms

Scenarios	Diesel generator in service	Demand loads		Wind power (MW) / Number of states	
		P (MW)	Q (MVAr)	Wind farm in service	Wind farm out of service
SP	#1, #2, #5 - #10	74.807	7.849	10.2/340	0/130
SL	#1, #2, #5 - #7	31.967	-4.458	10.2/292	0/82
WP	#1, #2, #5 - #9	62.291	6.654	10.2/324	0/114
WL	#1, #2, #5 - #7	31.444	1.371	10.2/292	0/82

Table 2: Number of system state variables, demand loads, operational diesel generators, and wind power generation under variant scenarios

IV. Simulation Results

The above-mentioned operating scenarios with a varying penetration of wind power were investigated and compared to the cases with only synchronous generators in operation. Eigenvalue analysis under different wind penetration levels was implemented to investigate the dynamic behavior in the Penghu power system. The diesel generator is modeled with a six order state equation, state variables $x = [\text{psie}, \text{psiD}, \text{psiX}, \text{psiQ}, \text{speed}, \text{phi}]$. The excitors of the generators #1-#4 and generators #5-#12 are modeled with a six and a five order state equations, state variables $x = [x_a, x_b, x_e, x_{f1}, x_{f2}, x_r]$ and $x = [x_a, x_{der}, x_e, x_i, x_r]$, respectively. The speed governor is modeled with a six state equation, state variables $x = [x_1, x_2, x_4, x_5, x_6]$. The wind turbine with full-load converter is modeled with a fifteen order state equation, including the states of the PQ, current and over frequency power reduction controllers. The detailed representation of the state variables can be found in [14]. Simulations were realized using DIgSILENTPowerFactory 15.1 software [15].

4.1 Eigenvalues

Small signal stability analysis identifies the causes of poorly damped or unstable power system oscillations and provides effective means for oscillation damping control. Eigenvalue analysis, based on the computation of the critical eigenvalues and corresponding eigenvectors of the system state matrix, gives this kind of information for the analysis and control of the small signal stability of the system. In this study, the eigenvalue analysis has been carried out for the Cases SP, SL, WP, and WL in the Penghu power system, and all eigenvalues have negative real parts, which indicated that the Penghu power system is inherently dynamically stable under different scenarios. The plots of obtained eigenvalues are shown in Fig. 2. Comparing Fig. 2-(a) with 2-(b) of each study case shows that eigenvalues associated with the dynamics of full-load converter wind turbines are actually fast decay modes, i.e. eigenvalues with larger negative real parts. It means that the dynamics of full-load converter wind turbines has relatively limited contribution to the low frequency oscillations.

The critical eigenvalues associated with the dominant oscillatory modes, also known as low frequency oscillatory modes, for the Cases SP, SL, WP, and WL are summarized in Tables 3-6. Results show that all oscillation modes have damping ratios larger than 13%, and only five oscillating modes with damping ratios between 13% and 20% in each study case. It means that the Penghu power system is a well damped system, whether the wind farms are in service or not. The observation can be drawn that the Penghu power system operating on light load has larger damping ratio than that operating on peak load, and the presence of the full-load converter wind turbines has less impact on the damping of low frequency oscillations.

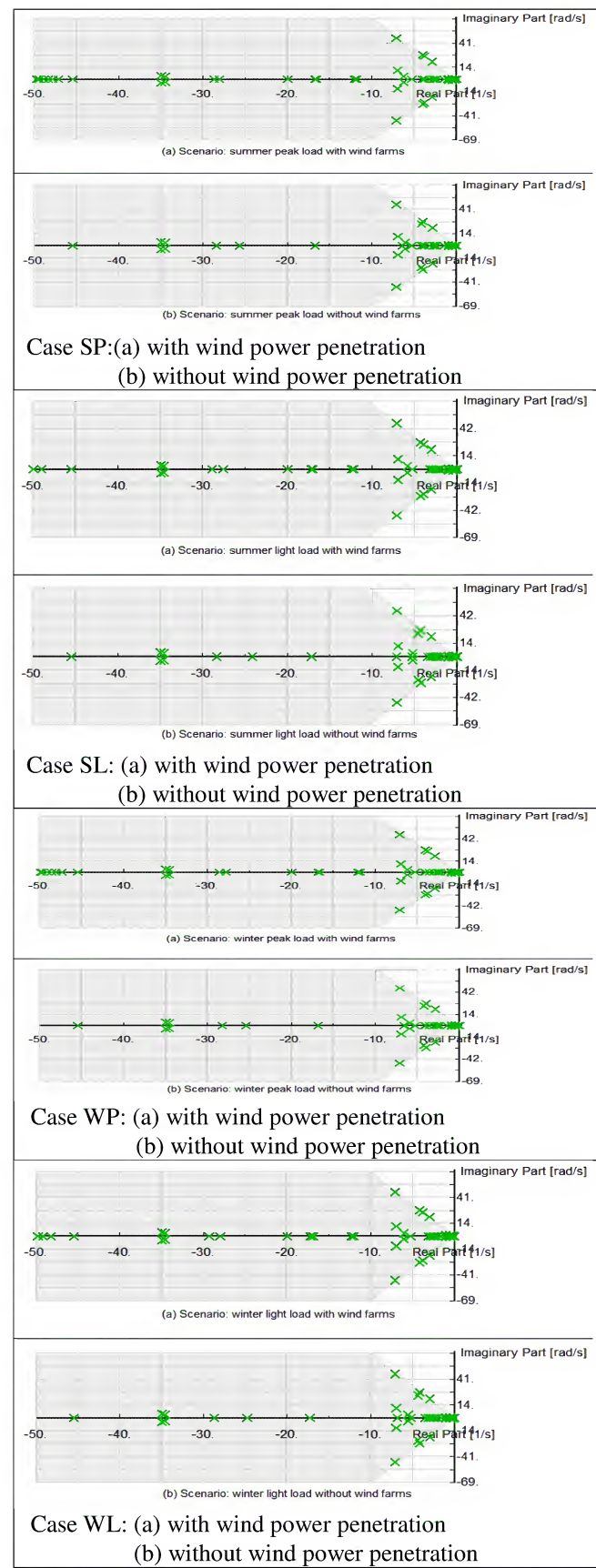


Fig. 2: Eigenvalues with/without wind power penetration under different scenarios

Scenario	Eigenvalue	Oscillation frequency, Hz	Damping ratio
Summer peak loadwith wind farm penetration	-2.86359± j20.32880	3.23543	0.13949
	-3.96518± j28.02058	4.45961	0.14011
	-3.77347± j26.64261	4.24030	0.14023
	-7.10147± j46.98080	7.47727	0.14946
	-0.09439± j0.33881	0.05392	0.26836
Summer peak loadwithout wind farm penetration	-2.84443± j20.36390	3.24101	0.13834
	-3.92909± j27.39341	4.39163	0.14097
	-7.10153± j49.98051	7.47718	0.14946
	-4.17473± j24.90488	3.96374	0.16532
	-0.09539± j0.33791	0.05378	0.27168

Table 3: Dominant oscillatory modes for Case SP

Scenario	Eigenvalue	Oscillation frequency, Hz	Damping ratio
Winter peak loadwith wind farm penetration	-2.88423± j20.37619	3.24297	0.14015
	-3.79408± j26.26862	4.18078	0.14295
	-4.02150± j27.84183	4.43117	0.14296
	-7.10151± j46.98026	7.47714	0.14946
	-0.09394± j0.34369	0.05470	0.26366
	-2.86366± j20.41291	3.24882	0.13893
Winter peak loadwithout wind farm penetration	-3.98314± j27.37512	4.35689	0.14399
	-7.10159± j46.97990	7.47708	0.14946
	-4.23051± j24.52102	3.90264	0.17001
	-0.09508± j0.34301	0.05459	0.26713

Table 5: Dominant oscillatory modes for Case WP

Scenario	Eigenvalue	Oscillation frequency, Hz	Damping ratio
Summer light loadwith wind farm penetration	-3.06665± j20.36862	3.24177	0.14888
	-7.10204± j46.97479	7.47627	0.14949
	-3.95243± j25.26231	4.02062	0.15458
	-4.29631± j27.33522	4.3505	0.15527
	-0.09909 ± j0.35009	0.05572	0.27232
Summer light loadwithout wind farm penetration	-3.04624± j20.40272	3.24720	0.14767
	-7.10224± j46.97429	7.47619	0.14950
	-4.26421± j26.6704	4.24473	0.15788
	-4.54704± j23.38833	3.72237	0.19084
	-0.10195± j0.35501	0.05650	0.27601

Table 4: Dominant oscillatory modes for Case SL

Scenario	Eigenvalue	Oscillation frequency, Hz	Damping ratio
Winter light load with wind farm penetration	-2.97120± j20.52730	3.26721	0.14324
	-4.13310± j27.84249	4.43127	0.14684
	-3.81696± j25.65823	4.08364	0.14714
	-7.10202± j46.97406	7.47616	0.14949
	-0.10771± j0.35992	0.05728	0.28670
Winter light load without wind farm penetration	-2.96103± j20.55013	3.27065	0.14262
	-7.10217± j46.97371	7.47610	0.14950
	-4.12252± j27.14895	4.32089	0.15013
	-4.35863± j23.88378	3.80122	0.17953
	-0.10886± j0.36414	0.05796	0.28642

Table 6: Dominant oscillatory modes for Case WL

4.2 Participation factors

Low frequency oscillatory modes, usually including inter-area and local-area modes, can be identified by the concepts of frequency of oscillation, mode shapes and participation factors. The participation factors of a mode indicate the contribution of the system state variables to the mode. According to the equation (4), participation factors of a critical oscillation mode were calculated with the critical eigenvalues and corresponding left and right eigenvectors of the system state matrix, which were based on the four scenarios as shown in Table 2. In each scenario, the Penghu power system connected with and without wind farms were considered. The results have been shown in Figs 3-6 and Table 7.

Figs 3-6 show that the participation factors associated with the most critical eigenvalue have their magnitudes larger than 0.1, and are clustered within 30 degrees in each group for each study case. Results indicate that the main contribution of the oscillations is the state variables associated with the dynamics of the synchronous generators in Chien-shan power plant. It presents a local electromechanical mode, and is mainly associated with generator speed (speed), rotor position angle (phi), and flux in Q-damper winding (psiQ) transients.

In Table 7, comparing the penetration factors with and without wind farms penetration for each study case shows that all of the state variables associated with the full-load converter interfaced wind turbines do not contribute to the local electromechanical mode, it means that the configuration in the full-load converter wind turbine has the ability to decouple the wind generator dynamics from the gird dynamics.

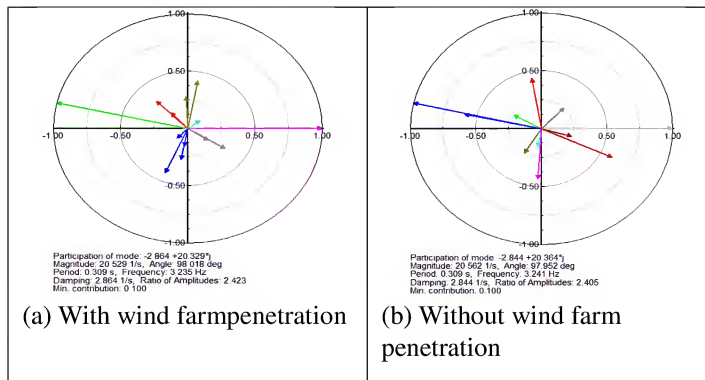


Fig. 3: Comparison of the participation factors of the critical eigenvalue for case SP

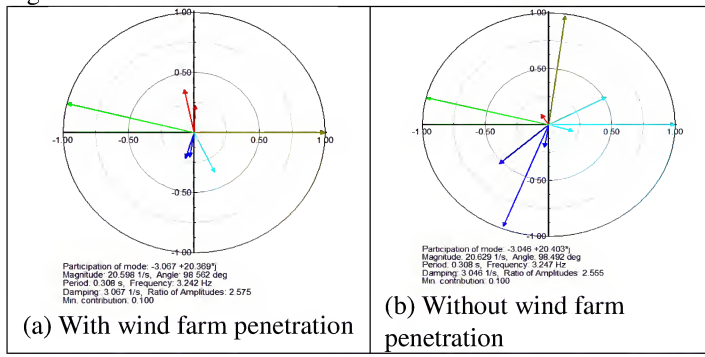


Fig. 4: Comparison of the participation factors of the critical eigenvalue for case SL

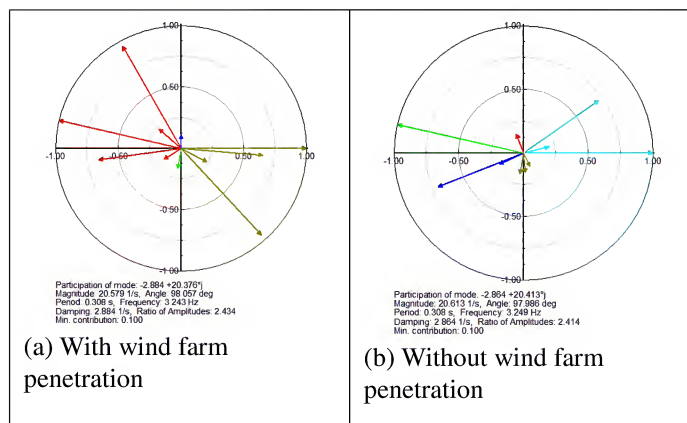


Fig. 5: Comparison of the participation factors of the critical eigenvalue for case WP

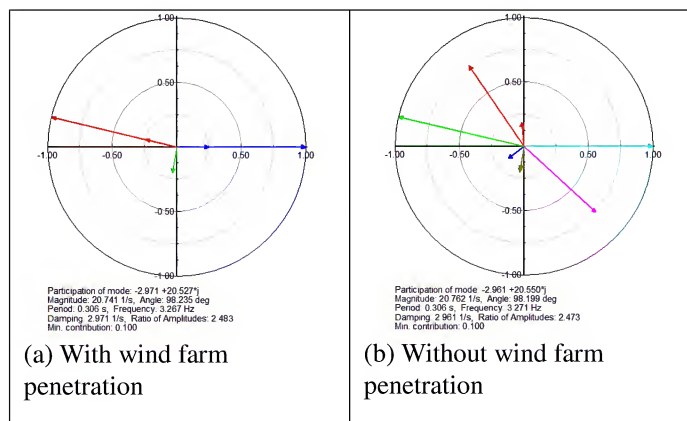


Fig. 6: Comparison of the participation factors of the critical eigenvalue for case WL

V. Conclusion

The small signal stability of the wind farm integrated power system was examined. Based on the eigenvalue and participation factor computation, the simulation with various wind penetration levels and wind turbine with full-load converter was conducted to examine the low frequency oscillations of the Penghu power system. The simulation results show that the eigenvalues associated with the dynamics of the synchronous generators are the mainly local electromechanical modes, whereas those with full-load converter wind turbines are actually fast decay modes and thus have less impact on the damping of low frequency oscillations.

VI. Acknowledgment

Financial support by the Ministry of Science and Technology of the R.O.C. is gratefully acknowledged (Grant No. MOST 104-2221-E-146-005).

Cluster	State Variable	Participation Magnitude	Participation Angle (deg)	Cluster	State Variable	Participation Magnitude	Participation Angle (deg)
Case SP with WFs: $\lambda = -2.86359 \pm j20.32880$				Case SP without WFs: $\lambda = -2.84443 \pm j20.36390$			
1	G5_phi_1	0.331	134.471	1	G10; speed	0.439	99.486
	G6_phi_3	0.185	132.385		G7; phi	0.996	167.181
2	G9; phi	0.996	167.051	2	G9; speed	0.596	168.115
	G10; phi_8	0.419	-113.044		G6; phi	0.238	151.461
3	G7; phi_5	0.276	-100.118		G10; phi_7	0.437	-93.331
	G9; psiQ_0	0.159	-99.141	3	G8; speed	0.249	-121.47
	G8; speed_7	0.114	-131.273		G7; psiQ_9	0.158	-99.055
4	G10; speed_1	0.421	79.905	4	G8; phi	0.248	45.707
	G7; speed_3	0.277	92.831		G7; speed	1	0
5	G8; phi_3	0.114	35.778	5	G9; phi	0.594	-24.702
6	G9; speed	1	0		G6; speed	0.239	-15.719
7	G5; speed_1	0.332	-32.581				
	G6; speed_9	0.185	-34.666				
Case SL with WFs: $\lambda = -3.06665 \pm j20.36862$				Case SL without WFs: $\lambda = -3.04624 \pm j20.40272$			
1	G5_phi_8	0.365	101.679	1	G6; psiQ	0.107	122.923
	G7; speed_2	0.225	87.3925	2	G7; phi	0.995	166.149
2	G6; phi_0	0.995	166.011		G5; phi	0.975	-111.48
3	G7; phi_1	0.224	-106.595	3	G6; speed	0.522	-137.89
	G6; psiQ_5	0.206	-99.269		G7; speed	0	3
4	G6; speed	1	0		G7; psiQ	0.205	-99.182
5	G5; speed_7	0.367	-64.332	4	G5; speed	0.980	82.361

Case WP with WFs: $\lambda = -2.88423 \pm j20.37619$				Case WP without WFs: $\lambda = -2.86366 \pm j20.41291$			
	G5; phi_5	0.996	166.979	1	G8; speed	0.158	109.321
	G9; phi_3	0.951	119.184	2	G9; phi	0.996	167.119
1	G7; speed_6	0.659	-171.884		G6; phi	0.712	-157.79
	G6; phi_3	0.235	138.202	3	G7; speed	0.206	-153.96
	G9; psiQ_1	0.160	-146.878		G9; psiQ	0.167	-98.992
2	G5; psiQ_7	0.167	-99.082	4	G8; phi	0.158	-83.559
3	G7; psiQ_6	0.110	89.032		G6; psiQ	0.119	-63.901
	G5; speed_1	1	0				
4	G9; speed	0.954	-47.795	5	G6; speed	0.714	35.090
	G7; phi_5	0.657	-4.904		G7; phi	0.206	13.157
	G6; speed_1	0.236	-28.777				
Case WL with WFs: $\lambda = -2.97120 \pm j20.52730$				Case WL without WFs: $\lambda = -2.96103 \pm j20.55013$			
	G5; phi_9	0.994	166.648		G6; phi_8	0.755	124.189
1	G6; phi_8	0.248	166.562	1	G5; speed_0	0.185	95.037
	G7; phi_8	0.248	166.562	2	G7; phi_3	0.995	166.728
2	G5; psiQ_1	0.205	-98.820	3	G6; psiQ_3	0.154	-141.34
	G5; speed_1	1	0	4	G7; psiQ_2	0.203	-98.810
3	G6; speed_8	0.249	-0.0322		G5; phi_2	0.184	-98.233
	G7; speed_8	0.249	-0.0322	5	G7; speed_0	1	0

Table 7: Participation factors and associated state variables of the critical eigenvalue for each Case: SP, SL, WP, and WL under with/without wind farms penetration

VII. References

- i. The Global Wind Energy Council, Retrieved from <http://www.gwec.net/>
- ii. Heier, S.(2006). Grid Integration of Wind Energy Conversion Systems. England: John Wiley & Sons Ltd.
- iii. Slootweg, J. G., Ploinder H.,& Kling W.L.(2001). Initialization of wind turbine models in power system dynamics simulations. IEEE Porto Power Tech Conference, 10th-13th, September, Porto, Portugal.
- iv. Mei, F., & Pal, B.C.(2005). Modelling and small-signal analysis of a grid connected doubly-fed induction generator. Power Engineering Society General Meeting, 2101-2108.

- v. Mishra, Y., Mishra, S., & Li, F.(2009). Small-signal stability analysis of a DFIG-based wind power system under different modes of operation. *IEEE Transactions on Energy Conversion*, 24(4), 972-982.
- vi. Li, S.Y., Wu, T., Li, Q.J., & Liu, H.(2010). Analysis of small signal stability of grid- connected doubly fed induction generators. *Power and Energy Engineering Conference*, 28th-31st, March, 1-4.
- vii. Mehta, B., Bhatt, P., & Pandya, V.(2014). Small signal stability analysis of power systems with DFIG based wind power penetration. *Electrical Power and Energy Systems*, 58(2014), 64-74.
- viii. Yang, L., Yang, G.Y., Xu, Z., Dong, Z.Y., Wong, K.P., & Ma, X.(2010). Optimal controller design of a doubly-fed induction generator wind turbine system for small signal stability enhancement. *IET Gener. Transm. Distrib.*, 4(5), 579-597.
- ix. Wu, F., Zhang, X.P., & Ju, P.(2009). Small signal stability analysis and control of the wind turbine with the direct-drive permanent magnet generator integrated to the grid. *Electric Power Systems Research*, 79(2009), 1661-1667.
- x. Knuppel, T., Nielsen, J.N., Jensen, K.H., Dixon, A., & Ostergaard, J.(2010). Small signal stability of wind power system with full-load converter interfaced wind turbines. *IET Renewable Power Generation*, 6(2), 79-91.
- xi. Huang, H., Mao, C., Lu, J., & Wang, D.(2012). Small-signal modelling and analysis of wind turbine with direct drive permanent magnet synchronous generator connected to power grid. *IET Renewable Power Generation*, 6(1), 48-58.
- xii. Samanvorakij, S., & Kumkratug, P.(2013). Modeling and simulation PMSG based on wind energy conversion system in MATLAB/SIMULINK. *Proc. of the Second Intl. Conf. on Advances in Electronics and Electrical Engineering-AEEE2013*, 37-41.
- xiii. Kundur, P.(1994). *Power System Stability and Control*. New York, USA: McGraw-Hill, Inc.
- xiv. DIgSILENTPowerFactory 15.1 User Manual, Retrieved from <http://www.digsilent.de/>
- xv. DIgSILENT GmbH, Retrieved from <http://www.digsilent.de/>